

A novel approach for the definition of small-field sizes using the concept of superellipse

I. Méndez^{*}, B. Casar

Department of Dosimetry and Quality of Radiological Procedures, Institute of Oncology Ljubljana, Zaloška cesta 2, Ljubljana, 1000, Slovenia

ARTICLE INFO

Keywords:

Superellipse
Small fields
Output factors
Radiochromic film dosimetry

ABSTRACT

In radiotherapy, field sizes are defined in terms of the dimensions of the irradiation area. However, geometric square fields result in irradiation areas with rounded corners, which become almost elliptical for small fields. Superellipses are a family of curves encompassing shapes lying between ellipses and rectangles. The purpose of this work was to analyze the advantages and disadvantages of a novel approach that describes small-field sizes with superellipses. Square fields with nominal side lengths ranging from 0.5 to 10 cm were irradiated with two different linacs using 6 and 10 MV photon beams with and without flattening filters. Field size dimensions and output factors were measured by employing radiochromic films and the Radiochromic.com software. An alternative definition of equivalent square small-field size based on the superellipse (S_{se}) was introduced. The degree n of the superellipse for 10 cm nominal fields measured between 14.8 ± 1.0 to 27.7 ± 1.9 . However, it decreased with the field size, down to between 2.26 ± 0.10 and 2.64 ± 0.15 for 0.5 cm nominal side lengths. A relation between the degree n and the equivalent square small-field size (S_{clin}) as defined by Cranmer-Sargison et al. ["A methodological approach to reporting corrected small field relative outputs," *Radiotherapy and Oncology* 109, 350–355 (2013)] was found. For nominal side lengths of 10 cm, S_{se} was between $0.34 \pm 0.04\%$ and $0.10 \pm 0.01\%$ smaller than S_{clin} , while for 0.5 cm nominal side length S_{se} was between $9.5 \pm 0.6\%$ and $7.4 \pm 0.7\%$ smaller than S_{clin} . There was no significant difference in the goodness of the regression between using S_{se} or S_{clin} to fit field output factors with the function proposed by Sauer and Wilbert. Small fields were found to be more accurately characterized with superellipses. The advantages and disadvantages of describing field sizes with superellipses were examined. Field output factors can be derived with equivalent square small-field sizes based on the superellipse approach.

1. Introduction and purpose

Widely implemented radiotherapy techniques, such as intensity-modulated radiation therapy (IMRT), volumetric modulated arc therapy (VMAT), and stereotactic radiosurgery (SRS), among others, rely on small fields for dose delivery by linear accelerators. Due to the clinical importance of accurate small-field dosimetry, a large number of studies have been published on the subject. However, in many cases, it was not possible to compare their results easily since the researchers used different definitions for small-field sizes. To avoid confusion and ambiguity in the interpretation of the reported results, the latest international dosimetry protocol IAEA TRS-483 (Palmans et al., 2017), published jointly by IAEA and AAPM, and dedicated entirely to the dosimetry of small fields of megavoltage photon beams, provided clear recommendations on the definition of small-field sizes.

According to the International Electrotechnical Commission, the projection of the collimator aperture defines the geometrical field size, while the irradiation field size is defined in terms of the dimensions of the area outlined by a specified isodose perpendicular to the axis of the beam (IEC, 2004). In broad beams, geometrical field sizes correspond to irradiation field sizes when measuring the full width at half maximum (FWHM) of the lateral beam profile (*i.e.*, the 50% isodose) at the isocentre depth. In small fields, though, the irradiation field delimited by the 50% isodose is larger than the geometrical field size. This apparent field widening is due to the partial occlusion of the primary photon source and loss of lateral charged particle equilibrium (LCPE) (Palmans et al., 2017, 2018) on the beam axis.

In IAEA TRS-483, the field size represents the irradiation field size defined by the FWHM of the lateral beam profile at a depth enough to eliminate contaminating electrons – 10 cm depth is recommended. The

^{*} Corresponding author.

E-mail address: nmendez@onko-i.si (I. Méndez).

<https://doi.org/10.1016/j.radphyschem.2021.109775>

Received 15 December 2020; Received in revised form 7 June 2021; Accepted 29 June 2021

Available online 7 September 2021

0969-806X/© 2021 The Authors. Published by Elsevier Ltd. This is an open access article under the CC BY license (<http://creativecommons.org/licenses/by/4.0/>).

irradiation area is characterized by the in-plane and cross-plane dimensions in rectangular fields, and by the radius in circular fields.

Equivalent square field sizes are widely used in radiation therapy to derive dosimetric properties of fields with non-square shapes (Xiao et al., 1999; Venselaar et al., 1997; Day, 1972; Sterling, 1964). For the determination of field output factors, IAEA TRS-483 follows the definition of equivalent fields proposed by Cranmer-Sargison et al. (2013). Equivalent square small-field sizes (S_{clin}) are based on equal area of field sizes:

$$S_{clin} = \sqrt{AB} \quad (1)$$

where A and B stand for cross-plane and in-plane dimensions, respectively, for rectangular fields, and

$$S_{clin} = r\sqrt{\pi} \quad (2)$$

where r is the radius of the field, for circular fields.

However, square fields produce, in fact, irradiation areas with rounded corners, which give small fields near-elliptic shapes. Irradiation fields of square, rectangular, and circular geometrical fields are better described by superellipses, a family of curves that encompass ellipses and rectangles (Fig. 1). In addition to in-plane and cross-plane dimensions, superellipses require a third term called *degree* (n), and satisfy the equation:

$$\left| \frac{x}{A/2} \right|^n + \left| \frac{y}{B/2} \right|^n = 1 \quad (3)$$

where n , A and B are positive numbers.

The area of the superellipse mirrors the area of a rectangle multiplied by a correction in terms of the gamma function, $\Gamma(x)$, and the degree:

$$\text{Area} = AB \frac{\left(\Gamma\left(1 + \frac{1}{n}\right) \right)^2}{\Gamma\left(1 + \frac{2}{n}\right)} \quad (4)$$

The purpose of this work was to analyze the advantages and disadvantages of describing field sizes with superellipses, and to propose an alternative definition of equivalent square small-field sizes based on

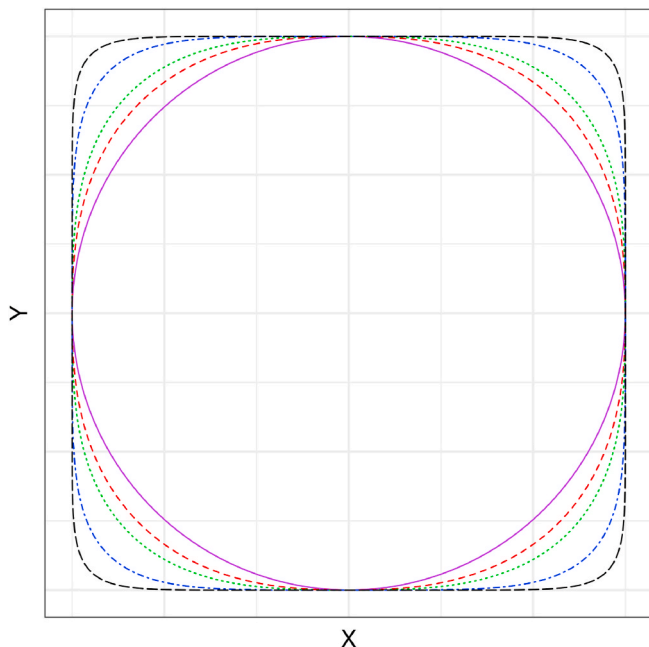


Fig. 1. Examples of superellipses, with $n = 2$ (purple color, solid line), 2.5 (red, dashed), 3 (green, dotted), 5 (blue, dotdash), 10 (black, logdash).

superellipses.

2. Methods and materials

2.1. Experimental measurements

Experimental measurements were taken in two different hospitals, one equipped with an Elekta Versa HD (Elekta AB, Stockholm, Sweden) linear accelerator with Agility MLC system, and the other equipped with a Varian TrueBeam (Varian Medical Systems, Palo Alto, CA, USA) with Millennium MLC system. For each linear accelerator, flattening filter (WFF) and flattening filter free (FFF) photon beams of energies 6 and 10 MV were measured. We will denote them as 6 MV WFF, 6 MV FFF, 10 MV WFF, and 10 MV FFF. For each beam, nine square fields with nominal side lengths of 0.5, 0.8, 1.0, 1.5, 2.0, 3.0, 4.0, 5.0, and 10.0 cm were irradiated. Measurements were made employing an isocentric setup at 90 cm source-to-surface distance (SSD) and 10 cm depth.

Field sizes and output factors were measured with radiochromic films. Films were placed in a RW3 Solid Water phantom (PTW Freiburg, Freiburg, Germany) for the Elekta Versa HD linac and in a Virtual Water phantom (Standard Imaging Inc, Middleton, WI, USA) for the Varian TrueBeam linac. Three measurements with different film fragments were performed for each combination of beam energy and field size. Gafchromic EBT3 films (Ashland Inc., Wayne, NJ, USA) from lots 04071601 and 06291702 were used for the Elekta and Varian linacs, respectively. Films were scanned before and after irradiation (Méndez, 2015) to reduce uncertainties. A flatbed scanner Epson Expression 10000XL (Seiko Epson Corporation, Nagano, Japan) was used for the films irradiated with the Elekta linac and an Epson Expression 11000XL scanner for the Varian linac. Scans were taken in reflection mode with 150 dpi resolution (i.e., 0.17 mm/px) and 48-bit RGB mode (16 bit per channel). The scan software was Epson Scan v3.49a in both cases. Additional details on the measurements can be found in earlier publications (Casar et al., 2019, 2020).

2.2. Calculations

Film scans were processed with a research version of Radiochromic.com v3.3 software (Radiochromic SL, Benifaió, Spain). Inter-scan and lateral corrections were applied, and doses were obtained with the Multigaussian dosimetry model (Mendez et al., 2018, 2021). For each film fragment, the field central dose was calculated as the mean dose value in a circular region of interest (ROI) with 0.5 mm of diameter centered on the irradiation field size. The center of the field was obtained with an iterative algorithm. Starting from the approximate position of the center, the algorithm located the contour of the 50% isodose of the central dose. Then, the center of the isodose became the new center of the field, and a new contour was located. This loop was repeated ten times, even though it converged much earlier to displacements of the center smaller than the resolution of the image. Once the position of the center was known, the irradiation field size was shaped by the last detection of the 50% isodose. The field size contour was fitted according to equation (3) by means of a genetic algorithm. The parameters to fit were the rotation of the superellipse, cross-plane (A) and in-plane (B) dimensions, and the degree (n) of the superellipse.

In this work, all uncertainties are reported with coverage factor $k = 2$. For each film fragment, Type B uncertainties of the field dimensions and the degree of the superellipse were estimated conservatively. The uncertainty of field dimensions was estimated as 0.14 mm assuming that field boundaries follow a uniform probability density function with the resolution of the scan as base. The uncertainty of the degree (n) was estimated as 4%, and was derived by bootstrap resampling each point of the field boundary. Type A uncertainties were obtained from statistical analysis of the repeated measurements of each field.

Central dose uncertainties (always with $k = 2$) were estimated as 3.4% for Elekta Versa HD fields and 4.4% for Varian TrueBeam fields by

combining intra-fragment uncertainty, inter-fragment uncertainty, and intra-lot variations with respect to the calibration.

Equivalent square small-field sizes based on the approach followed by Cranmer-Sargison et al. (S_{clin}) were calculated following equation (1). Equivalent square small-field sizes based on the superellipse (S_{se}) were defined and calculated as the square root of equation (4), that is:

$$S_{se} = \sqrt{AB} \frac{\Gamma\left(1 + \frac{1}{n}\right)}{\sqrt{\Gamma\left(1 + \frac{2}{n}\right)}} \quad (5)$$

The variation of the degree n as a function of field size was analyzed, as well as the relative difference ($\delta_{se/clin}$) in equivalent square small-field size between S_{se} and S_{clin} defined as

$$\delta_{se/clin} = 100 \frac{S_{se} - S_{clin}}{S_{clin}}. \quad (6)$$

Uncertainties of S_{clin} were calculated by propagation of uncertainty. Uncertainties of S_{se} and $\delta_{se/clin}$ were obtained by parametric bootstrap resampling.

Field output factors as a function of equivalent square small-field size – either S_{clin} or S_{se} in this work – were computed for each linear accelerator and beam energy. They were fitted with the analytical function proposed by Sauer and Wilbert (2007):

$$\Omega(s) = P_{\infty} \frac{s^m}{l^m + s^m} + S_{\infty} (1 - e^{-bs}), \quad (7)$$

where $\Omega(s)$ stands for the field output factor as a function of the equivalent square field size, P_{∞} is the maximum primary dose, S_{∞} is the maximum scatter component, and m , l , and b are fitting parameters. The effect of using S_{se} instead of S_{clin} for the determination of field output factors was evaluated.

3. Results

3.1. Irradiation fields as superellipses

Superellipses with circular and elliptical shapes have degree n equal to two, while larger degrees produce shapes closer to rectangles. Fig. 2 displays some examples of field contours and superellipse fittings for different nominal field sizes and beam energies. Field contours are not continuous lines as a consequence of film uncertainties and pixel dimensions. In Fig. 3, the degrees of the superellipses obtained by fitting

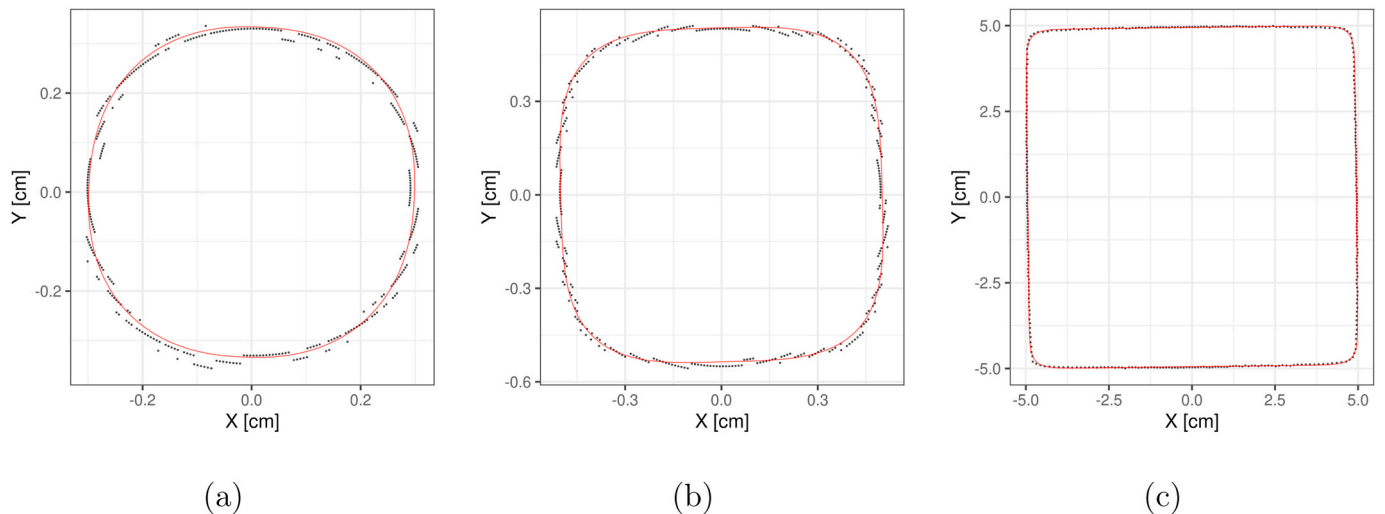


Fig. 2. Field contours (50% isodoses, as black dots) and superellipse fittings (as red lines) of nominal fields a) 0.5 cm 10 MV WFF, b) 1 cm 6 MV WFF, and c) 10 cm MV FFF, all of them irradiated with Elekta Versa HD.

the irradiation fields measured for each film, nominal field size, beam energy, and linear accelerator are plotted as a function of equivalent square small-field size S_{clin} . Field sizes with nominal side length of 10 cm had n values going from 14.8 ± 1.0 (Varian 10 MV FFF) to 27.7 ± 1.9 (Varian 6 MV WFF), which means that they are rectangular in shape with rounded corners. However, degrees n decreased with the field size, leading to n values going from 2.26 ± 0.10 (Elekta 6 MV WFF) to 2.64 ± 0.15 (Varian 10 MV FFF) for nominal side lengths of 0.5 cm. Uncertainties of S_{clin} are not plotted because they were too small. All of them were between 0.01 and 0.02 cm except for one field that was 0.04 cm (Elekta 10 MV FFF). Uncertainties of S_{se} were slightly different, but also were between 0.01 and 0.02 cm except for the uncertainty of the Elekta 10 MV FFF field, which was 0.04 cm.

Fig. 3 also shows the regression of the degree n of the superellipse as a function of S_{clin} . The fitting function was considered to be a second degree polynomial:

$$n(S_{clin}) = \alpha S_{clin}^2 + \beta S_{clin} + \gamma. \quad (8)$$

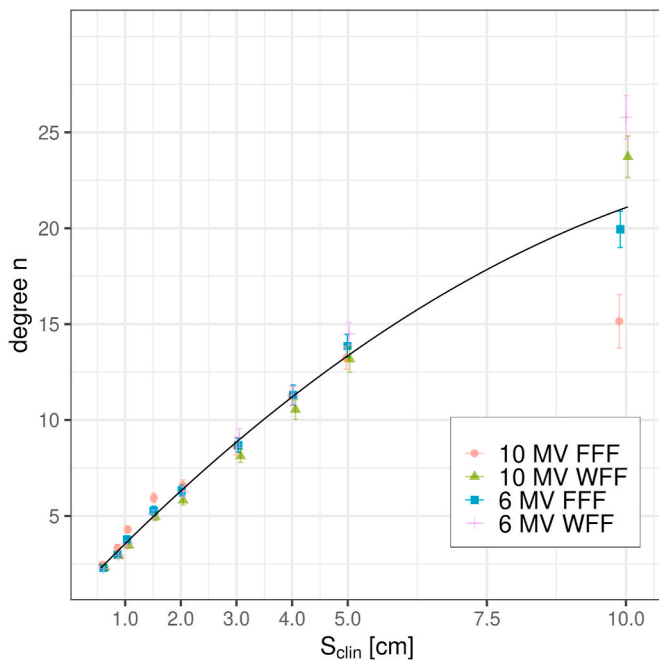
The values of the fitting parameters are presented in Table 1 as a function of linac and energy. Since linac and energy interaction terms were found not significant ($p > 0.05$), the fitting parameters of all measures aggregated are included too. The regression line plotted in Fig. 3 uses the fitting parameters of all measures aggregated.

3.2. Difference between S_{clin} and S_{se}

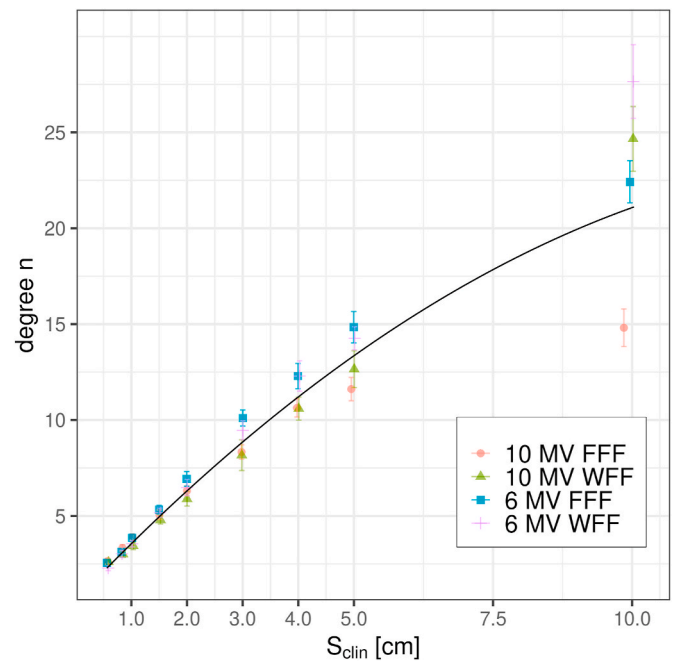
Fig. 4 shows the relative difference in equivalent square small-field size between S_{se} and S_{clin} as a function of S_{clin} for both linacs. For nominal side lengths of 10 cm, the difference went from $-0.34 \pm 0.04\%$ (Varian 10 MV FFF) to $-0.10 \pm 0.01\%$ (Varian 6 MV WFF), while for nominal side lengths 0.5 cm the difference went from $-9.5 \pm 0.6\%$ (Elekta 6 MV WFF) to $-7.4 \pm 0.7\%$ (Varian 10 MV FFF). The line resulting from calculating S_{se} with the parameters of $n(S_{clin})$ from Table 1 is also plotted.

3.3. Field output factors

The effect on the computation of field output factors when using the superellipse instead of the Cranmer-Sargison et al. approach is shown in Fig. 5. As mentioned before, the difference in terms of equivalent square small-field size went approximately from 0.2 mm for 10 cm nominal side length to 0.5 mm for 0.5 cm. The shift in equivalent square small-field size was similar for all beam energies in both linacs. Hence, to avoid



(a)



(b)

Fig. 3. Degree n of the superellipse as a function of equivalent square small-field size S_{clin} for a) Elekta Versa HD and b) Varian TrueBeam photon beams, and regression line.

Table 1

Regression of the degree n as a function of S_{clin} : values of the fitting parameters of equation (8) and coefficient of determination.

Linac	Energy	α	β	γ	R^2
Elekta Versa HD	6 MV WFF	-0.05 ± 0.03	3.0 ± 0.2	0.5 ± 0.2	0.998
Elekta Versa HD	6 MV FFF	-0.13 ± 0.04	3.3 ± 0.2	0.3 ± 0.2	0.996
Elekta Versa HD	10 MV WFF	-0.03 ± 0.03	2.6 ± 0.2	0.7 ± 0.2	0.997
Elekta Versa HD	10 MV FFF	-0.22 ± 0.07	3.6 ± 0.4	0.5 ± 0.4	0.989
Varian TrueBeam	6 MV WFF	-0.04 ± 0.02	3.0 ± 0.2	0.5 ± 0.2	0.999
Varian TrueBeam	6 MV FFF	-0.12 ± 0.03	3.5 ± 0.2	0.4 ± 0.2	0.998
Varian TrueBeam	10 MV WFF	-0.00 ± 0.03	2.3 ± 0.2	1.1 ± 0.2	0.997
Varian TrueBeam	10 MV FFF	-0.161 ± 0.015	2.99 ± 0.12	0.97 ± 0.12	0.999
All linacs	All energies	-0.10 ± 0.03	3.1 ± 0.2	0.6 ± 0.2	0.972

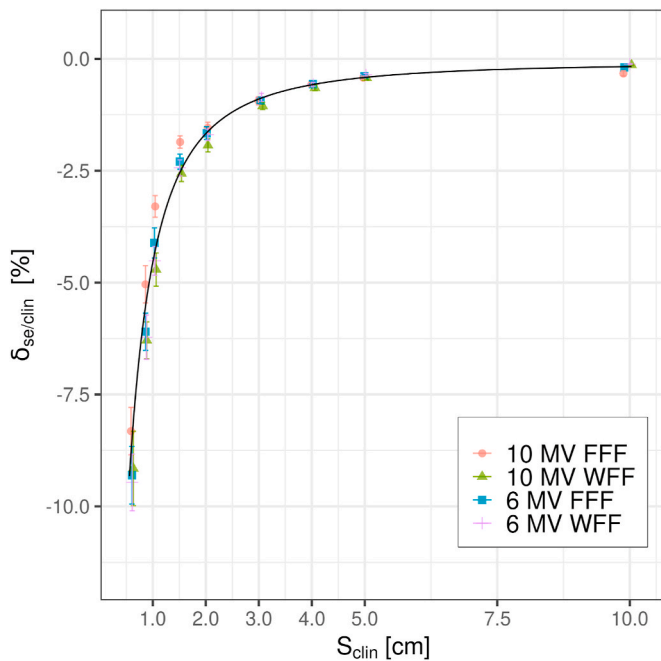
redundancies, only the graph with 10 MV WFF from the Elekta Versa HD linear linac is shown as an example.

The ability of equation (7) to fit field output factors as a function of S_{se} was subject to scrutiny. In Table 2, the residual standard errors of fitting field output factors as a function of equivalent square small-field sizes (either S_{clin} or S_{se}) with equation (7) are shown. The residuals were weighted with the inverse of the square of the uncertainty of the output factors. The relative likelihood of using S_{clin} or S_{se} to fit field output factors was calculated with the Akaike Information Criterion statistic and it was found that the differences between both models were not significant.

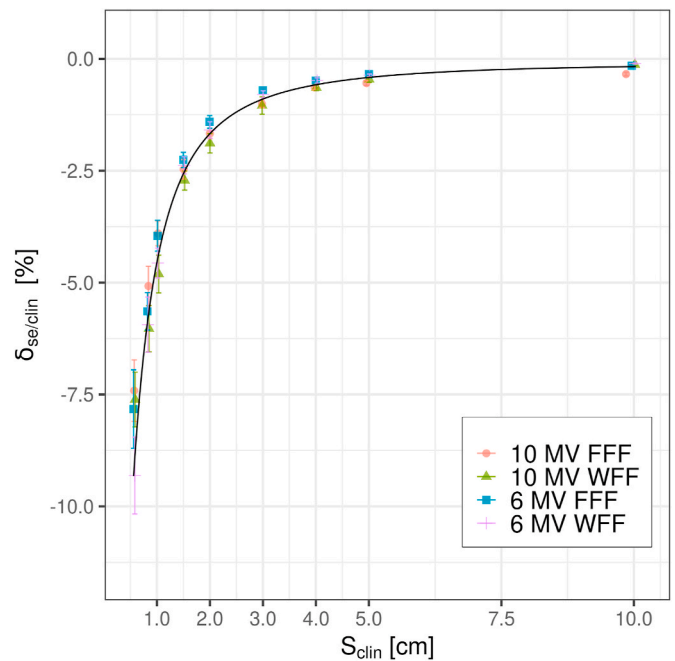
4. Discussion

Currently, the adopted and recommended approach to describe irradiation areas of nominally square small-fields of MV photon beams uses only the in-plane and cross-plane dimensions (Palmans et al., 2017). Yet, as shown in Fig. 3, they are better characterized as superellipses, requiring the degree n as an additional, third parameter. Another advantage of considering field sizes as superellipses is that geometrical square, rectangular and circular field sizes are all handled uniformly. For instance, equivalent square small-field sizes can be defined by equation (5) in all cases. When field dimensions are measured with a 2D detector, the superellipse approach has the additional benefit of using the whole isodose contour to calculate the parameters of the field. Even though this is a disadvantage in terms of complexity because it demands a computer program to obtain the dimensions, it provides more accurate results. This is especially important for measurements with radiochromic films, which are a convenient dosimeter for small-fields measurements (Palmans et al., 2017; Casar et al., 2019) but suffer from heterogeneities (Mendez et al., 2018). Nevertheless, superellipses can still be used to fit the whole isodose contour even if equivalent square small-field sizes are defined according to the method introduced by Cranmer-Sargison et al. In this case, in-plane and cross-plane dimensions are recorded, while the degree n is disregarded.

The main difficulty with superellipses is that they cannot be (easily) measured with 1D detectors. However, with the experimental data set obtained in this study, equation (8) could be used to derive the degree n as a function of S_{clin} when square small fields are measured with 1D detectors. Equation (8) is a rough model of the relationship between n and S_{clin} . For instance, a more realistic model should take into account that n is expected to monotonically increase with S_{clin} . Yet, as shown in Fig. 4, equation (8) becomes meaningless for fields larger than 10 or even 5 cm, since, for fields larger than 5 cm, the difference between S_{clin} and S_{se} may be considered negligible for most applications. Therefore, even though there are significant differences between the values of degree n for FFF and WFF beams with 10 cm nominal side length - n is



(a)



(b)

Fig. 4. Relative difference $\delta_{se/clin}$ in equivalent square small-field size between S_{se} (superellipse approach) and S_{clin} (Cranmer-Sargisson et al. approach) as a function of S_{clin} for a) Elekta Versa HD and b) Varian TrueBeam photon beams, and regression line.

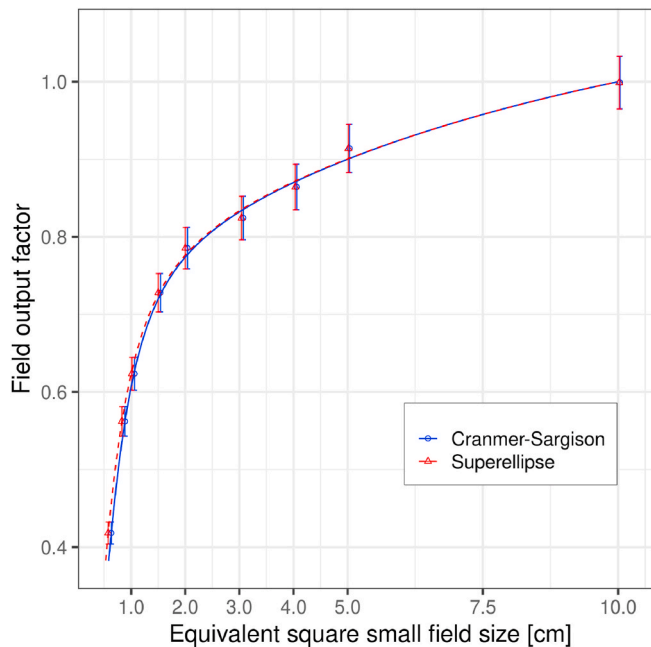


Fig. 5. Field output factors as a function of equivalent square small-field size, defined with the Cranmer-Sargisson et al. (S_{clin}) and superellipse (S_{se}) approach for 10 MV WFF generated by Elekta Versa HD linac.

significantly lower for 10 MV FFF than for 10 MV WFF beams and for 6 MV FFF than for 6 MV WFF beams for both linacs, which can be explained by the more circular nature of FFF beams - these differences lead to negligible differences in terms of field size.

Field output factors can be interpolated from equation (7) with equivalent square small-field sizes calculated either by the Cranmer-Sargisson et al. method or by the superellipse method. The only

Table 2

Residual standard errors of fitting field output factors as a function of equivalent square small-field size (either S_{clin} or S_{se}) with equation (7).

Linac	Elekta Versa HD		Varian TrueBeam	
	S_{clin}	S_{se}	S_{clin}	S_{se}
6 MV WFF	1.043	1.048	0.609	0.611
6 MV FFF	1.038	1.015	0.518	0.520
10 MV WFF	0.731	0.745	0.865	0.876
10 MV FFF	1.079	1.068	0.928	0.923

requirement is that a consistent approach is followed for the sample of fields measured to obtain the fitting parameters, as well as for the fields being interpolated. It is especially important not to mix both definitions of equivalent square small-field sizes, since it can result in 10% changes in field output factors for the smallest fields. If a consistent definition is observed, dose or clinical differences between using S_{clin} or S_{se} should be minor for geometrical square fields, since not significant differences were found between fitting field output factors with S_{clin} or S_{se} . For non-square small fields, the dosimetric impact of the superellipse approach remains open for further research.

5. Conclusions

Small fields of MV photon beams are currently described with the radius or with the width and length of the field. However, they can be more accurately characterized with superellipses. Superellipses are a family of curves including shapes lying between ellipses and rectangles. In this work, the advantages and disadvantages of a novel approach that describes field sizes with superellipses were analyzed. Also, an alternative definition of equivalent square small-field size based on the superellipse was proposed. The superellipse approach can be used to derive field output factors as a function of equivalent square small-field size using the function proposed by Sauer and Wilbert (2007).

Author statement

Description of the contributions of each author:

Ignasi Méndez: Conceptualization, Methodology, Investigation, Software, Formal analysis, Writing - Original Draft.

Božidar Casar: Methodology, Investigation, Writing - Review & Editing, Funding acquisition.

Declaration of competing interest

The authors declare that they have no known competing financial interests or personal relationships that could have appeared to influence the work reported in this paper.

Acknowledgments

The authors would like to thank Eduard Gershkevitsh and David Čugura for their assistance during the experimental part of the study. Božidar Casar acknowledges partial financial support from the Slovenian Research Agency through the research Grant P1-0389.

References

- Casar, B., Gershkevitsh, E., Méndez, I., Jurković, S., Huq, M.S., 2019. A novel method for the determination of field output factors and output correction factors for small static fields for six diodes and a microdiamond detector in megavoltage photon beams. *Med. Phys.* 46, 944–963.
- Casar, B., Gershkevitsh, E., Méndez, I., Jurković, S., Saiful Huq, M., 2020. "Output correction factors for small static fields in megavoltage photon beams for seven ionization chambers in two orientations—perpendicular and parallel. *Med. Phys.* 47, 242–259.
- Cranmer-Sargison, G., Charles, P.H., Trapp, J.V., Thwaites, D.I., 2013. A methodological approach to reporting corrected small field relative outputs. *Radiother. Oncol.* 109, 350–355.
- Day, M., 1972. The equivalent field method for axial dose determinations in rectangular fields. *Br. J. Radiol.* 11, 95–10.
- IEC, 2004. Medical Electrical Equipment – Glossary of Defined Terms. Standard IEC-60788. International Electrotechnical Commission, Geneva.
- Méndez, I., 2015. Model selection for radiochromic film dosimetry. *Phys. Med. Biol.* 60, 4089.
- Méndez, I., Polšak, A., Hudej, R., Casar, B., 2018. The multigaussian method: a new approach to mitigating spatial heterogeneities with multichannel radiochromic film dosimetry. *Phys. Med. Biol.* 63, 175013.
- Méndez, I., Rovira-Escutia, J.J., Casar, B., 2021. A protocol for accurate radiochromic film dosimetry using Radiochromic.com. *Radiol. Oncol.* 55 (3), 369–378.
- Palmans, H., Andreo, P., Huq, M.S., Seuntjens, J., Christaki, K., 2017. Dosimetry of Small Static Fields Used in External Beam Radiotherapy: an Iaea-aapm International Code of Practice for Reference and Relative Dose Determination. International Atomic Energy Agency, "Vienna.
- Palmans, H., Andreo, P., Huq, M.S., Seuntjens, J., Christaki, K.E., Meghzi, A., 2018. Dosimetry of small static fields used in external photon beam radiotherapy: summary of trs-483, the iaea-aapm international code of practice for reference and relative dose determination. *Med. Phys.* 45, e1123–e1145.
- Sauer, O.A., Wilbert, J., 2007. Measurement of output factors for small photon beams. *Med. Phys.* 34, 1983–1988.
- Sterling, T., 1964. Derivation of a mathematical expression for the percent depth dose of cobalt 60 beams and visualization of multiple fields dose distributions. *Br. J. Radiol.* 37, 544–550.
- Venselaar, J., Heukelom, S., Jager, H., Mijnheer, B., Van Gasteren, J., Van Kleffens, H., Van der Laarse, R., Westermann, C., 1997. Is there a need for a revised table of equivalent square fields for the determination of phantom scatter correction factors? *Phys. Med. Biol.* 42, 2369.
- Xiao, Y., Bjärngard, B., Reiff, J., 1999. Equivalent fields and scatter integration for photon fields. *Phys. Med. Biol.* 44, 1053.